

Metabolic remodelling in adipocytes promotes CNTF-mediated fat loss in obesity

Seamus Crowe¹, Sarah M. Turpin¹, Francine Ke¹, Bruce E. Kemp^{1,2} and Matthew J. Watt¹

¹St. Vincent's Institute of Medical Research and the Department of Medicine, The University of Melbourne;

²CSIRO Molecular Health Technologies, 343 Royal Parade, Parkville, Victoria, 3052, Australia.

Address for correspondence and reprints:

Matthew J. Watt, Ph.D.

Department of Physiology

Monash University

Clayton, Victoria

Australia 3800.

Ph: 61 3 9905 2584

Email: matthew.watt@med.monash.edu.au.

Running title: CNTF and adipocyte remodelling in obesity

Grants: Diabetes Australia Research Trust, Ramaciotti Foundation

Disclosure Statement: The authors have nothing to disclose

Abstract

Obesity is characterized by an expanded adipose tissue mass and reversing obesity reduces the risk of insulin resistance and cardiovascular disease. Ciliary neurotrophic factor (CNTF) reverses obesity by promoting the preferential loss of white adipose tissue. We evaluated the cellular and molecular mechanisms by which CNTF regulates adiposity. Obese mice fed a high fat diet were treated with saline (HFD) or recombinant CNTF for 10 days and adipose tissue was removed for analysis. Another group fed a HFD were pair fed (PF) to CNTF mice. In separate experiments 3T3-L1 adipocytes were treated with CNTF to examine metabolic responses and signaling. CNTF reduced adipose mass that resulted from reductions in adipocyte area and triglyceride content. CNTF treatment did not affect lipolysis but resulted in decreases in fat esterification and lipogenesis and enhanced fatty acid oxidation. The enhanced fat oxidation was associated with the expression of peroxisome proliferator-activated receptor coactivator1 α (PGC1 α) and nuclear respiratory factor 1, increases in oxidative phosphorylation subunits and mitochondrial biogenesis as determined by electron microscopy. Studies in cultured adipocytes revealed that CNTF activates p38 mitogen activated protein kinase and AMP activated protein kinase (AMPK). Inhibiting p38 activation prevented the CNTF-induced increase in *PGC1 α* but not AMPK activation. Diminished food intake with PF induced similar decreases in fat mass but this was related to increased expression of uncoupling protein 1. We conclude that CNTF re-programs adipose tissue to promote mitochondrial biogenesis, enhancing oxidative capacity and reducing lipogenic capacity, thereby resulting in triglyceride loss.

Key words: adipose tissue, cytokine signaling, fat oxidation, mitochondrial biogenesis

Obesity is characterised by increased fat deposition in visceral and subcutaneous depots and is an underlying feature of several related metabolic defects including insulin resistance, dyslipidemia, hypertension and cardiovascular disease (1). Central events in obesity development include defective adipose tissue lipolysis, increased lipogenesis and reduced oxidative capacity (2-5); however, the molecular and metabolic processes underpinning these defects are not fully understood.

Ciliary neurotrophic factor (CNTF) is a member of the gp130 receptor cytokine family identified as an anti-obesity agent in rodents and humans (6-10). CNTF administration induces rapid and pronounced loss of white adipose tissue. This weight loss is substantially attributable to reduced food intake, increased uncoupling of metabolism in brown adipose tissue and greater whole body energy expenditure (6); however, these effects do not explain the specific loss of white adipose tissue. CNTF effects persist for several days after cessation of treatment, indicating that transcriptional changes are also likely to mediate CNTF's anti-obesogenic effects. The CNTF receptor α is expressed in adipose tissue (11) and heterodimerizes with the transmembrane gp130 receptor upon activation. The gp130 receptor shares close sequence homology with the leptin receptor and contains a SH2 domain capable of activating the Jak/Stat signaling pathway following ligand binding. Interestingly, leptin overexpression by adenoviral administration markedly reduces adipose tissue mass by inducing mitochondrial biogenesis and converting white adipose into a tissue that partly resembles highly oxidative brown adipose tissue (12). Hyperleptinemia also increased fatty acid oxidation and was associated with AMP-activated protein kinase (AMPK) activation. We have previously demonstrated that CNTF activates AMPK and fatty acid oxidation in skeletal muscle, and that unlike leptin treatment, these effects persist in obesity (9).

The objective of the present study was to investigate the mechanisms underpinning the CNTF-induced adipose tissue loss. We hypothesized that CNTF induces mitochondrial biogenesis and enhances fatty acid oxidation in white adipose tissue, thereby reducing adiposity. To this end, we evaluated the acute and chronic effects of CNTF on adipose tissue morphology and metabolism. Since CNTF metabolic effects persist after the cessation of treatment (6, 13), we

also examined adipose tissue gene expression using an oligonucleotide microarray approach.

Research Design and Methods

Cell culture

3T3-L1 preadipocytes were grown in Dulbecco's modified Eagle's medium (DMEM) supplemented with 25 mmol/l glucose and 10% foetal bovine serum (FBS). Fibroblasts were grown to confluence and differentiation was induced by changing the culture medium to DMEM and 2% FBS containing Actrapid insulin (0.5 mU.ml⁻¹; Novo Nordisk), 0.1 μ g.ml⁻¹ dexamethasone, and 25 μ g.ml⁻¹ 3-Isobutyl-1-methylxanthine. Differentiating medium was removed after 3 days and replaced with DMEM in 5% FBS with 0.5mU/ml Actrapid insulin. The medium was then replaced every 2 days until cells were loaded with lipid droplets, usually after 8-10 days. For acute experiments, the cells were incubated overnight in DMEM and 0.5% FBS (no insulin) prior to stimulation with 10 ng/ml recombinant CNTF (CNTF_{Ax15}, kindly provided by Regeneron Pharmaceuticals). This dose does not induce inflammation in adipocytes (Figure 6A-C). For chronic treatment with CNTF (10 ng/ml), adipocyte media was replaced with fresh media every 24 h. For experiments involving p38 α / β inhibition, cells were pre-treated with 10 μ M SB202190 (Sigma Aldrich, St. Louis, MI) prior to the addition of 10 ng/ml CNTF. cDNAs encoding wild-type p38 MAPK and kinase-deficient p38 MAPK with a glutamate to alanine mutation at residue 168 (D168A), kindly provided by Dr. Gregory Steinberg (St. Vincent's Institute). For infection studies, differentiated 3T3-L1 adipocytes (day 7) were infected with adenovirus for 40 h, then incubated overnight in DMEM plus 0.5% serum prior to experiments. Oil Red O was used to quantify triglyceride mass as described (14).

Animals and animal care

Male C57Bl/6 mice were purchased from Monash Animal Services (Clayton, Victoria, Australia) at 8 weeks of age and placed on a standard chow diet consisting of 5% of calories from fat or a high-fat diet (HFD) consisting of 45% of calories from fat for 10 weeks. This experimental design was used to induce obesity in HFD mice. Animals were housed in a pathogen-free facility with a 12 h light / 12 h dark cycle and were given free access to food and water. All procedures were approved by the St. Vincent's Hospital Animal Experimentation Ethics Committee and were conducted in accordance with the National Health

and Medical Research Council of Australia Guidelines on Animal Experimentation.

Experimental Design

Mice were assigned to one of four experimental groups for the 10 day experimental period. Control chow fed (Con) and high-fat fed (HFD) mice were allowed *ad libitum* access to food. Another group of HFD animals was injected at 0800 daily with 0.3 mg/kg CNTF (CNTF), which was previously shown to induce weight loss without induction of an inflammatory response (7, 9). A third group of HFD were pair fed (PF) to mice in the HFD CNTF group to account for the suppression of food intake observed with CNTF administration. Animals were fasted for 4 h prior to experiments and were anaesthetized by intraperitoneal injection of sodium pentobarbital (60 mg/kg body mass). The epididymal fat pad was excised and weighed, then rinsed in phosphate buffered saline containing 0.1% bovine serum albumin (BSA) and dissected into 20-40 mg pieces for immediate functional analysis. The remaining tissue was fixed for morphological assessment or rapidly frozen for protein / mRNA analysis. A venous blood sample was obtained from the pleural cavity and the plasma was frozen for later analysis. Animals were sacrificed by lethal injection of sodium pentobarbital.

Adipose tissue lipolysis, oxidation and lipogenesis

For all experiments a modified Krebs's-Henseleit buffer was gassed for 40 min with 95% O₂ / 5% CO₂. Glucose (5 mM) and fatty acid free bovine serum albumin (BSA, 4%) was added to the buffer immediately prior to experiments. All experiments were conducted in a shaking water bath at 30°C.

Lipogenesis. D-[3-³H]glucose (Amersham, TRK239) was added to the buffer to give a final concentration of 0.5 µCi/ml. Adipose tissue explants were incubated for 2 h and the media was removed. The tissue was washed in phosphate buffered saline (PBS) then homogenized in 1 ml of PBS. The lipids were extracted in 2:1 chloroform: methanol, a 1 ml aliquot of the organic phase was removed, scintillation fluid added and radioactivity was counted in a liquid scintillation analyser.

Lipolysis. Adipose tissue explants were placed in 2 ml buffer. The media was collected after 2 h for later determination of glycerol by an enzymatic colorimetric method (Sigma).

Oxidation. Palmitate oxidation was assessed over 5 h by radiometric methods as described previously for skeletal muscle (15).

Adipocyte area

Adipose tissue was immersed in Bouin's solution overnight then transferred to 70% ethanol and stored at 4°C. Tissues were fixed and embedded with a random orientation in paraffin and 10 µm sections were stained with hematoxylin and counterstained with eosin. For each sample, area was determined in 190 ± 9 adipocytes (obtained from 3 independent sections of tissue) at x 400 magnification using an Olympus BX50 (Olympus, Tokyo, Japan) microscope and AIS software (Ontario, Canada).

Electron microscopy and determination of mitochondria size and density

Adipose tissue was fixed in 2.5% glutaraldehyde in 0.1M cacodylate buffer (ph 7.4) at RT for 2 h and post-fixed in 2% osmium tetroxide solution for 1 h. After dehydrating in graded acetone, tissue was embedded in araldite/epon resin. Thick sections (0.5 µm) were performed using Ultracut S ultramicrotome (Leica, North Ryde, NSW, Australia) then stained with 1% methylene blue. Thin sections (90 nm) were cut using the same microtome mounted on copper/palladium 200 mesh grids then stained with 3% aqueous solution of uranyl acetate and lead citrate. Grids were examined in Siemens Elmiskop 102 electron microscope at 60 kV.

Immunoblotting

Adipose tissue was lysed and the homogenate was centrifuged at 14,000 x g for 30 min at 4°C. The supernatant containing cytosolic proteins was carefully removed, proteins were solubilised, subjected to SDS-PAGE and transferred onto PVDF membranes. Membranes were blocked in 5% skim milk and incubated for 1 h in primary antibody, washed and incubated with protein G-HRP. Primary antibodies for cytochrome C and OxPhos complexes were obtained from BioVision (Mountain View, CA) and Mito Sciences (Eugene, OR). The phospho-p38 MAPK antibody was from Cell Signaling (Beverly, MA, USA) and α-actin from Sigma-Aldrich. The immunoreactive proteins were detected by enhanced chemiluminescence and quantified by densitometry.

RNA extraction and real-time quantitative PCR

Total RNA was isolated from adipose tissue by QIAzol extraction and the RNeasy mini kit (Qiagen, Doncaster, Australia). Reverse transcription of mRNA was performed using the

thermoscript RT-PCR system (Invitrogen, Mount Waverly, Australia) with random hexamer priming. Quantitative real time PCR was performed on the Stratagene Mx3000p using Assay-on-Demand gene expression kits for mouse NRF-1, PGC1 α , CPT1, UCP1, UCP2, UCP3, GPAT, CD68, F4/80 and 18S (Applied Biosystems, Foster City, CA). cDNA was amplified using 20 μ l TaqMan PCR reactions containing 3 mM MgCl₂, 200 mM dNTP's, 100 nM primers, 50 nM TaqMan probe, 1 X Gold reaction buffer and 0.5 U Amplitaq gold (Applied Biosystems). Assays were performed in triplicate and normalized using 18s ribosomal RNA (Applied Biosystems). The relative quantities of each transcript were calculated using the comparative critical threshold (Ct) method.

DNA microarray

Affymetrix GeneChip technology was used (Affymetrix Inc., Santa Clara, California, USA) to determine gene expression changes at the genome level. RNA quality was assessed on an Agilent Bioanalyser Picochip. Samples were labeled and hybridized to the GeneChip Mouse Expression Set 430 2.0 following the manufacturer's protocols. The arrays were scanned on an Affymetrix GeneArray scanner. Data analysis was performed using Spotfire (Spotfire Inc, Somerville, MA, USA) and Ingenuity Pathways Analysis 5.5. Expression values for each gene were calculated using multi-array average. The false discovery rate adjusted to P<0.05.

Statistical analysis

Results are presented as the mean \pm standard error of the mean (SEM). Data were analyzed for differences by one way analysis of variance (ANOVA) with specific differences located with a Tukey's post hoc test. Statistical significance was set *a priori* at P<0.05 .

Results

CNTF decreases adiposity and adipocyte size in mice

CNTF and PF mice consumed less food (~40%) when compared with HFD mice (Table 1). Body mass was decreased by 14.9 \pm 1.1% and 16.7 \pm 1.4% in CNTF and PF after 10 days treatment (Table 1). Epididymal fat pad mass was increased in HFD vs Chow (Figure 1A). The epididymal fat mass was reduced by 32% and 43% in CNTF and PF, respectively, but remained heavier than Chow. Similar reductions occurred in retroperitoneal and subcutaneous tissue (data not shown). The average adipocyte area was greater in HFD vs Chow (Figure 1B) and was reduced in CNTF and

PF. A representative picture of epididymal adipose tissue is shown in Figure 1E. Consistent with the enlarged adipocyte area, triglyceride content was increased in HFD vs Chow and reduced by PF and to a greater degree in CNTF (Figure 1C). To explain the apparent mismatch in fat mass, adipocyte area and triglyceride content, we examined adipocyte number in a subset of animals (n=3 per group). Adipocyte number was higher in CNTF versus PF and Chow (2.49 \pm 0.23 $\times 10^6$ vs 2.13 \pm 0.29 $\times 10^6$ vs 1.88 \pm 0.12 cells/mg tissue, respectively). Leptin is exclusively produced by adipocytes and was markedly reduced in CNTF and PF mice, which is consistent with the reduced adiposity and smaller adipocytes (Figure 1D).

The frequency distribution of adipocytes by area was similar between Chow, CNTF and PF whereas adipose tissue from HFD possessed a greater abundance of larger adipocytes (Figure 1E). Close inspection revealed greater number of smaller adipocytes in CNTF (ie. <1000 μ m²), indicating the possibility of adipogenesis. Accordingly, we assessed known markers of adipocyte differentiation by qRT-PCR. *PPAR γ* (1.8-fold) and *C/EBP α* (1.6-fold) were elevated in CNTF compared with Chow, but were not different from other groups (Table 1).

Acute exposure to CNTF increases fatty acid oxidation in white adipose tissue

We next assessed the effects of acute CNTF administration on lipid metabolism in epididymal fat explants *ex vivo*. Under conditions where isoproterenol and insulin stimulated lipolysis and lipogenesis respectively CNTF did not affect lipolysis (Figure 2A) or lipogenesis (Figure 2B), but increased fatty acid oxidation by 48% (Figure 2C). We also repeated these experiments in 3T3-L1 adipocytes because adipose tissue contains several cell types in the stromovascular compartment, including macrophages. CNTF administration increased fatty acid oxidation by 20% in cultured adipocytes, an increment comparable to that seen when cells were treated with the AMPK pharmacological activator AICAR (5-aminoimidazole-4-carboxamide-1- β -D-ribofuranoside) (Figure 2D). The increase in fatty acid oxidation coincided with an increase in AMPK Thr172 (Figure 2E) and acetyl CoA carboxylase (ACC) Ser221 phosphorylation (Figure 2F), indicating activation of AMPK with CNTF. Because CNTF weight loss effects persist after cessation of treatment (6), we hypothesised that CNTF induces transcriptional responses that stably up-regulate fat oxidation. To test whether

prolonged CNTF treatment could enhance the fat oxidative capacity of the adipocyte independent of AMPK activation, 3T3-L1 adipocytes were treated with CNTF for three days and the media was removed 16 h prior to experiments. Fatty acid oxidation was increased by 23% in CNTF treated cells (Figure 2D). To test whether CNTF induces TG depletion independent of caloric intake and humoral factors, we incubated 3T3-L1 adipocytes (day 7) in CNTF containing media and assessed TG content by Oil Red O staining. Cells treated with CNTF exhibited a 12% reduction in TG content after only 3 days (Figure 2G). These data suggest that CNTF increases fat oxidation in adipocytes acutely by AMPK activation and chronically by enhanced fat oxidative capacity (eg: transcriptional effects) to reduce fat mass.

Chronic exposure to CNTF increases fatty acid oxidation and decreases lipogenesis in white adipose tissue

To examine whether these CNTF effects are maintained *in vivo*, we examined fatty acid metabolism in epididymal adipose explants obtained from mice treated for 10 days with daily CNTF injections. Adipose tissue was dissected 16 h after the last CNTF injection, thereby eliminating acute CNTF effects because the half-life of CNTF is ~45 min (6). Lipolysis was unaffected by HFD and CNTF, but was decreased with PF (Figure 3A). Lipogenesis was decreased in CNTF compared with all groups without (Figure 3B) and with insulin stimulation (insulin-stimulated lipogenesis fold-change over basal: Chow, 4.9; HFD, 3.8; PF, 4.1; CNTF, 4.4). Thus, sensitivity to insulin was maintained in the CNTF treated animals. The incorporation of exogenous ¹⁴C-palmitate into triglycerides (ie: esterification) was decreased in CNTF compared with PF (caloric restricted) and tended to be lower than HFD (P=0.061, Figure 3D). Fatty acid oxidation was markedly increased in CNTF-treated mice compared with all groups (Figure 3D). These results suggest that chronic CNTF treatment enhances fatty acid oxidation and that this may reflect altered enzymatic regulation that with a net effect of directing fats towards oxidation rather than esterification and/or mitochondrial biogenesis.

CNTF induces mitochondrial biogenesis

The mitochondrial expression pattern was altered in adipose tissue following CNTF treatment. Electron microscopy revealed that mitochondrial number was increased by >50% with CNTF compared with all groups (Figure 4A); however, the size of individual mitochondria in CNTF were

not different from Chow or HFD (mitochondrial area, Figure 4B). The average area of individual mitochondria was increased in PF mice. The overall mitochondrial mass, calculated as the product of number and area, was 3.17, 2.55, 3.02 and 5.43 arbitrary units for Chow, HFD, PF and CNTF, respectively (P<0.05 CNTF vs. all other groups by one-way ANOVA), indicating that the total mitochondrial mass was increased by 2-fold in CNTF vs HFD. Consistent with these morphological changes, CNTF induced stable increases in nuclear respiratory factor (NRF-1) and PGC1 α (peroxisome proliferator-activated receptor γ coactivator 1 α) mRNA, both master regulators of mitochondrial biogenesis (Figure 4C and 4D). Carnitine palmitoyl transferase (CPT) 1 mRNA expression was also increased with CNTF (Figure 4E), indicating an enhanced potential for mitochondrial transport of long chain fatty acids, whereas medium chain acyl CoA dehydrogenase (MCAD) was not different between groups (not shown). We also examined mitochondrial proteins by Western blot. Adipose tissue from CNTF treated mice had increased protein expression of cytochrome c (electron transport chain protein), ATP synthase α and OxPhos Complex II (30 kDa Ip subunit) (Figure 4F-H)

PGC1 α activates expression of UCP1 (16), which is a protein that is highly expressed in brown adipose tissue and is characterized by a high oxidative capacity. UCP1 expression was low in white adipose tissue for all groups. Despite increasing PGC1 α mRNA, CNTF treatment did not enhance UCP1. UCP1 was elevated 2-fold in adipose of PF mice compared with all groups (Table 1). UCP2 and 3 were not different between groups (Table 1). Collectively, these data demonstrate that CNTF induces mitochondrial biogenesis in adipose tissue of mice, but does not enhance the capacity for uncoupled respiration. Conversely, pair feeding appears to induce adipose tissue loss, at least partially, via increased uncoupling.

p38 MAPK is required for CNTF-induced PGC1 α expression

To determine whether the CNTF effects on PGC1 α were specific, and not due to secondary events such as changes in circulating hormones / cytokines (9), we examined gene expression in cultured adipocytes after 5 h and 3 d of CNTF treatment. CNTF increased PGC1 α mRNA content after 5 h, and this was maintained at 3 days (P=0.055; Figure 5A). No effects were seen in 18S and Stat3 expression indicating some specificity in this response (Stat3 mRNA, P=0.88

by one-way ANOVA). To examine the upstream signaling events in CNTF-induced mitochondrial biogenesis, we examined known signalling events that upregulate PGC1 α mRNA, including p38 MAPK (17) and AMPK (18) 16 h after the final CNTF injection and observed no differences between groups (data not shown). Because CNTF is rapidly cleared (6), we next examined the acute effects of CNTF in 3T3-L1 adipocytes. CNTF increased p38 MAPK and AMPK Thr172 phosphorylation after 30 min (Figure 5B) and this effect was maintained at 4 h (not shown). However, in experiments where the culture media was replaced 30 min after the addition of CNTF, the effects observed on p38 MAPK and AMPK phosphorylation were not detected at 4 h, indicating that CNTF signaling to these kinases is transient. p38 MAPK and AMPK activation was not due an autocrine response to IL-6 as no changes in IL-6 mRNA or IL-6 release into the culture media were detected at 8 or 24 h after CNTF administration (Figure 6A). Proinflammatory cytokines such as IL-1 α , TNF α and IL-6 can activate p38 MAPK (19, 20); therefore, to determine whether p38 MAPK was required for the increase in PGC1 α mRNA, we pre-incubated cells with the p38 α / β inhibitor SB202190 for 30 min prior to the addition of CNTF. SB202190 totally blocked the CNTF-mediated increase in p38 MAPK phosphorylation (Figure 5C) but did not affect AMPK Thr172 phosphorylation (Figure 5C). PGC1 α mRNA expression was increased two-fold with CNTF; however, inhibiting p38 MAPK phosphorylation completely blocked these effects (Figure 5D). These findings were largely replicated in experiments where CNTF-induced p38 MAPK activation was inhibited by using a p38 MAPK dominant negative adenovirus (Figure 5B) and the expected rise in PGC1 α mRNA expression was suppressed (Figure 5E). These results show that CNTF-induced PGC1 α transcription depends on p38 signaling.

CNTF reduces the lipogenic capacity of white adipose tissue

Our *ex vivo* studies demonstrated reduced lipogenesis and esterification with CNTF, independent of reductions in food intake (Figure 3). To broadly determine the molecular mechanisms underpinning these responses, we probed for differential gene expression using cDNA microarrays on tissues obtained from mice placed on a high fat diet and treated with CNTF and PF controls. Comparative analysis of gene expression revealed that genes associated with fatty acid transport (FAT/CD36, FAS) triglyceride

synthesis (GPAT, DGAT) and lipogenesis (SCD1) were markedly downregulated with CNTF treatment (Table 2). These findings were validated by qRT-PCR for FAT/CD36, GPAT and SCD1. When 3T3-L1 adipocytes were treated with CNTF for 5 days, there was no change in FAS (-30% P=0.42), FAT/CD36 (-38% P=0.57), GPAT (+40% P=0.76) and SCD1 (-2% P=0.96), suggesting that the suppressive effects of CNTF on lipogenic gene expression *in vivo* may be mediated by a circulating / neural factor. These *in vitro* data contrast an earlier study showing reduced FAS and SREBP-1 protein expression following 96 h CNTF treatment in adipocytes (11).

CNTF does not attenuate obesity-induced macrophage infiltration into adipose tissue

It is well documented that obesity is associated with increased macrophage infiltration in to adipose tissue (21). To test whether CNTF-mediated reductions in adiposity were associated with reduced macrophage infiltration, we measured the macrophage specific markers CD68 and F4/80 by qRT-PCR. Both CD68 and F4/80 expression were increased 2-fold in adipose tissue with HFD; however, reducing adiposity with CNTF or PF did not reduce the expression of these macrophage markers (Table 1).

Discussion

Obesity is a major risk factor for several metabolic disorders including insulin resistance and type 2 diabetes. The use of CNTF for the treatment of obesity has been established (8-10); however, the cellular and molecular mechanism/s by which CNTF induces white adipose tissue loss is not completely clear (11). We describe how CNTF induces mitochondrial biogenesis to enhance fat oxidation within adipose tissue, via a process involving p38 MAPK activation and PGC1 α expression. The work presented also indicates that CNTF reduces the capacity for lipogenesis and fat re-esterification. Together, CNTF converts white adipose tissue towards a partial brown adipocyte phenotype and accordingly directs fatty acids towards oxidation rather than storage.

Mitochondrial capacity is an important determinant of tissue health. Obesity and type 2 diabetes are characterized by decreased mitochondrial gene expression (22, 23), reduced mitochondrial density (24) and reduced ATP turnover (25) in skeletal muscle. This contributes to an inability to efficiently oxidize fatty acids and results in excess fat deposition in this tissue.

There are now reports of defective mitochondrial function in adipose tissue in obesity/type 2 diabetes. Mitochondrial content and oxygen consumption are reduced in the adipose tissue of genetic (3, 4, 26, 27) and fat-induced obesity (26), suggesting that this may be a primary defect underpinning these conditions. It is also evident that insulin-sensitizing therapies, such as thiazolidinedione administration (2-4, 26) and PPAR α agonists (28), induce mitochondrial biogenesis and enhance fat oxidation (28) in white adipose tissue and may be implicit in the success of these strategies. In this report, we have identified two mechanisms capable of enhancing fat oxidation in adipocytes. Firstly, CNTF promoted fat oxidation acutely via activation of AMPK, which is consistent with our previous observations in skeletal muscle (9). Secondly, prolonged CNTF administration induced mitochondrial biogenesis, increased the expression of fat oxidative and respiratory chain proteins and enhanced fat oxidation, independent of acute AMPK activation. CNTF induces many of the metabolic changes seen in adenovirus induced hyperleptinemia including upregulation of PGC1 α but not UCP-1 and UCP-2. In contrast to hyperleptinemic rats that lose almost all of their adipose triglyceride mass and develop a fatless, hypervascular fat pad remnant, CNTF treated animals displayed smaller adipocytes and reduced triglyceride mass but retained normal morphology. Such regulated adipose loss, rather than complete adipose ablation, is important because the absence of adipose tissue (lipodystrophy) results in hepatomegaly, hypertriglyceridemia and disordered glucose metabolism leading to type 2 diabetes (29).

PGC1 α is a transcriptional coactivator that is involved in the upregulation of fatty acid oxidation genes and mitochondrial biogenesis and its activation has been linked with insulin sensitization (30). PGC1 α expression is reduced in the adipose tissue of obese (31) and type 2 diabetes patients (2), implicating PGC1 α in the pathogenesis of these metabolic disorders. Several studies have indicated that the 'conversion' of white to brown adipocytes is a viable strategy for the control of adiposity, and that PGC1 α is central to this approach. This is based on the rationale that brown adipose possesses a large mitochondrial mass and increased UCP1 expression, which results in greater fat metabolism and uncoupled respiration. In support of this premise, stable overexpression of PGC-1 α in 3T3-L1 adipocytes induced mitochondrial biogenesis (16) and adenoviral mediated PGC1 α

overexpression in white adipocytes induced changes consistent with brown adipocytes (32). Moreover, increased PGC1 α expression occurs in several rodent models with reduced adiposity including 4E-BP1 null mice (33), transgenic mice with activated polyamide catabolism (34) and as mentioned hyperleptinemic rats (12). While the molecular control of adipocyte mitochondrial biogenesis is unresolved, our data indicate that PGC1 α is involved in driving the CNTF-induced increase in mitochondrial biogenesis. The results also indicate that p38 MAPK signalling is involved as pharmacological and adenoviral inhibition of its activation inhibited CNTF stimulation of PGC1 α expression. It is unlikely that AMPK is important for this process because its activation and PGC1 α transcription were dissociated by p38 inhibition. Thus, besides CNTF inducing mitochondrial biogenesis, these studies support the intriguing possibility that an inability to efficiently oxidize fatty acids within adipose tissue may contribute to hypertrophy of adipose tissue and that enhancing fat oxidation within adipocytes may be a therapeutic strategy for obesity and related disorders.

Cytokines are known to regulate PGC1 α via p38 activation and increase the expression of genes linked to mitochondrial uncoupling and energy expenditure (19). An unexpected finding of the present study was the absence of UCP1 induction with CNTF, as UCP1 is a known downstream target of PGC1 α (16) and CNTF was shown previously to increase UCP1 and enhance thermogenesis in brown adipose tissue (6). Our findings of mitochondrial biogenesis and altered fuel metabolism, without UCP1 induction, indicate a partial shift from a white to brown adipose tissue phenotype. A dissociation between PGC1 α control and UCP1 expression was previously reported in β -adrenoceptor knockout brown adipocytes (35) and UCP1 expression was decreased in the absence of β 3-adrenoceptor agonism in brown adipocytes (36). Future studies are required to delineate in more detail the dissociation observed here.

Aside from enhanced fat oxidation, CNTF reduced lipogenesis and fat esterification. These physiological changes can be explained by stable CNTF-mediated transcriptional reprogramming. Notably, the CNTF-mediated changes inhibited key proteins of several pathways involved in lipogenesis including FAT/CD36, which is involved in fatty acid uptake, GPAT and DGAT, which are key proteins involved in glycerolipid synthesis, FAS, which catalyses *de novo* synthesis

of long-chain fatty acids from acetyl-CoA, malonyl-CoA and NADPH and SCD1, which is a rate-limiting enzyme in the synthesis of unsaturated fats (Figure 7). These findings extend on a previous report demonstrating decreased lipogenic gene expression in the liver with CNTF treatment (8). Pck1 encodes phosphoenolpyruvate carboxykinase which produces glycerol-3-phosphate as a precursor for fatty acid esterification into triglycerides. Interestingly, Pck1 was downregulated by CNTF and is noteworthy because increasing Pck1 may underpin the adiposity observed with PPAR γ agonists (37). Thus, CNTF is able to induce insulin sensitization (9, 10) without the weight gain observed with other traditional insulin sensitizers such as thiazolidinediones.

Fasting and CNTF induced a similar loss of adipose tissue. While this suggests that the reduced caloric intake is driving the adipose loss, an important point is that adipose loss was achieved through different mechanisms. Fasting was associated with increased plasma fatty acid levels and expression of UCP1, which is likely to promote uncoupled respiration and create a negative energy balance in this tissue. Fat specific over expression of UCP1 is known to reduce subcutaneous fat in aP2-Ucp1 transgenic mice (38). In contrast, CNTF reduced fatty acid synthesis and promoted fat oxidation, without evidence of uncoupling.

An abundance of evidence demonstrates a close link between obesity, chronic inflammation and insulin resistance (39). A recent advance in the understanding of obesity-induced inflammation and insulin resistance was the finding that the source of inflammatory cytokines in obesity is related to the number of resident macrophages in adipose tissue. Furthermore, the percentage of macrophages in a given adipose tissue depot is positively correlated with adiposity and adipocyte size (21, 40). However, recent studies suggest that macrophage infiltration is not necessarily a function of fat mass *per se*, and may be a reflection of adipose quality (41); a finding supported by the observation that macrophage infiltration is related to adipocyte death (42). The present *in vivo* data

indicate that while CNTF reduces adiposity, it does not affect the relative expression of adipose tissue macrophages (ATM) with high-fat feeding. This may have occurred because ATM turnover is relatively slow in mice fed high-fat diets (43). Alternatively, CNTF is known to induce proinflammatory signalling, which would presumably enhance ATM infiltration. This is unlikely because the concentrations of CNTF used in the *in vivo* studies do not induce an inflammatory or febrile response (9), observations supported by our *in vitro* analysis (Figure 6). Also, adipose tissue insulin sensitivity, as assessed by insulin-stimulated lipogenesis, was restored in CNTF treated animals, suggesting that the proportion of ATMs may not be an important factor determining insulin sensitivity or that CNTF may alter the properties of ATMs.

In conclusion, these studies advance the understanding of the treatment of obesity by identifying CNTF as a direct regulator of adipose tissue metabolism. The present study provides compelling evidence linking CNTF administration to mitochondrial biogenesis and transcriptional reprogramming resulting in enhanced fat oxidative and downregulated fat synthesis capacities. It remains to be determined whether approaches targeting gp130 signaling will be efficacious anti-obesity therapies in humans.

Acknowledgments

We thank Regeneron Pharmaceuticals for kindly supplying the CNTF_{Ax15}. We thank Drs Yuan Zhang and Darren Kelley for expert assistance with microscopy and Prof. Rick Kraemer (Stanford University) for advice on adipose tissue preparations. This study was supported by the Diabetes Australia Research Trust and the Ramaciotti Foundation. SMT is supported by a National Health and Medical Research Council (NHMRC) Dora Lush postgraduate scholarship, BEK is supported by an Australian Research Council Federation Fellowship and MJW is supported by a R Douglas Wright fellowship from the NHMRC.

References

1. **Zimmet P, Alberti KG, Shaw J** 2001 Global and societal implications of the diabetes epidemic. *Nature* 414:782-787
2. **Bogacka I, Xie H, Bray GA, Smith SR** 2005 Pioglitazone induces mitochondrial biogenesis in human subcutaneous adipose tissue in vivo. *Diabetes* 54:1392-1399
3. **Choo HJ, Kim JH, Kwon OB, Lee CS, Mun JY, Han SS, Yoon YS, Yoon G, Choi KM, Ko YG** 2006 Mitochondria are impaired in the adipocytes of type 2 diabetic mice. *Diabetologia* 49:784-791
4. **Wilson-Fritch L, Nicoloso S, Chouinard M, Lazar MA, Chui PC, Leszyk J, Straubhaar J, Czech MP, Corvera S** 2004 Mitochondrial remodeling in adipose tissue associated with obesity and treatment with rosiglitazone. *J Clin Invest* 114:1281-1289
5. **Arner P** 2005 Human fat cell lipolysis: biochemistry, regulation and clinical role. *Best Pract Res Clin Endocrinol Metab* 19:471-482
6. **Bluher S, Moschos S, Bullen J, Jr., Kokkotou E, Maratos-Flier E, Wiegand SJ, Sleemann MW, Mantzoros CS** 2004 Ciliary neurotrophic factorAx15 alters energy homeostasis, decreases body weight, and improves metabolic control in diet-induced obese and UCP1-DTA mice. *Diabetes* 53:2787-2796
7. **Lambert PD, Anderson KD, Sleeman MW, Wong V, Tan J, Hjarunguru A, Corcoran TL, Murray JD, Thabet KE, Yancopoulos GD, Wiegand SJ** 2001 Ciliary neurotrophic factor activates leptin-like pathways and reduces body fat, without cachexia or rebound weight gain, even in leptin-resistant obesity. *Proc Natl Acad Sci U S A* 98:4652-4657
8. **Sleeman MW, Garcia K, Liu R, Murray JD, Malinova L, Moncrieffe M, Yancopoulos GD, Wiegand SJ** 2003 Ciliary neurotrophic factor improves diabetic parameters and hepatic steatosis and increases basal metabolic rate in db/db mice. *Proc Natl Acad Sci U S A* 100:14297-14302
9. **Watt MJ, Dzamko N, Thomas WG, Rose-John S, Ernst M, Carling D, Kemp BE, Febbraio MA, Steinberg GR** 2006 CNTF reverses obesity-induced insulin resistance by activating skeletal muscle AMPK. *Nat Med* 12:541-548
10. **Gloaguen I, Costa P, Demartis A, Lazzaro D, Di Marco A, Graziani R, Paonessa G, Chen F, Rosenblum CI, Van der Ploeg LH, Cortese R, Ciliberto G, Laufer R** 1997 Ciliary neurotrophic factor corrects obesity and diabetes associated with leptin deficiency and resistance. *Proc Natl Acad Sci U S A* 94:6456-6461
11. **Zvonic S, Cornelius P, Stewart WC, Mynatt RL, Stephens JM** 2003 The regulation and activation of ciliary neurotrophic factor signaling proteins in adipocytes. *J Biol Chem* 278:2228-2235
12. **Orci L, Cook WS, Ravazzola M, Wang MY, Park BH, Montesano R, Unger RH** 2004 Rapid transformation of white adipocytes into fat-oxidizing machines. *Proc Natl Acad Sci U S A* 101:2058-2063
13. **Kelly JF, Elias CF, Lee CE, Ahima RS, Seeley RJ, Bjorbaek C, Oka T, Saper CB, Flier JS, Elmquist JK** 2004 Ciliary neurotrophic factor and leptin induce distinct patterns of immediate early gene expression in the brain. *Diabetes* 53:911-920
14. **Whitehead JP, Simpson F, Hill MM, Thomas EC, Connolly LM, Collart F, Simpson RJ, James DE** 2004 Insulin and oleate promote translocation of inosine-5' monophosphate dehydrogenase to lipid bodies. *Traffic* 5:739-749
15. **Pinnamaneni SK, Southgate RJ, Febbraio MA, Watt MJ** 2006 Stearoyl CoA desaturase 1 is elevated in obesity but protects against fatty acid-induced skeletal muscle insulin resistance in vitro. *Diabetologia* 49:3027-3037
16. **Puigserver P, Wu Z, Park CW, Graves R, Wright M, Spiegelman BM** 1998 A cold-inducible coactivator of nuclear receptors linked to adaptive thermogenesis. *Cell* 92:829-839
17. **Knutti D, Kressler D, Kralli A** 2001 Regulation of the transcriptional coactivator PGC-1 via MAPK-sensitive interaction with a repressor. *Proc Natl Acad Sci U S A* 98:9713-9718

18. **Jager S, Handschin C, St-Pierre J, Spiegelman BM** 2007 AMP-activated protein kinase (AMPK) action in skeletal muscle via direct phosphorylation of PGC-1alpha. *Proc Natl Acad Sci U S A* 104:12017-12022
19. **Puigserver P, Rhee J, Lin J, Wu Z, Yoon JC, Zhang CY, Krauss S, Mootha VK, Lowell BB, Spiegelman BM** 2001 Cytokine stimulation of energy expenditure through p38 MAP kinase activation of PPARgamma coactivator-1. *Mol Cell* 8:971-982
20. **Chan MH, McGee SL, Watt MJ, Hargreaves M, Febbraio MA** 2004 Altering dietary nutrient intake that reduces glycogen content leads to phosphorylation of nuclear p38 MAP kinase in human skeletal muscle: association with IL-6 gene transcription during contraction. *Faseb J* 18:1785-1787
21. **Weisberg SP, McCann D, Desai M, Rosenbaum M, Leibel RL, Ferrante AW, Jr.** 2003 Obesity is associated with macrophage accumulation in adipose tissue. *J Clin Invest* 112:1796-1808
22. **Kelley DE, He J, Menshikova EV, Ritov VB** 2002 Dysfunction of mitochondria in human skeletal muscle in type 2 diabetes. *Diabetes* 51:2944-2950
23. **Patti ME, Butte AJ, Crunkhorn S, Cusi K, Berria R, Kashyap S, Miyazaki Y, Kohane I, Costello M, Saccone R, Landaker EJ, Goldfine AB, Mun E, DeFronzo R, Finlayson J, Kahn CR, Mandarino LJ** 2003 Coordinated reduction of genes of oxidative metabolism in humans with insulin resistance and diabetes: Potential role of PGC1 and NRF1. *Proc Natl Acad Sci U S A* 100:8466-8471
24. **Ritov VB, Menshikova EV, He J, Ferrell RE, Goodpaster BH, Kelley DE** 2005 Deficiency of subsarcolemmal mitochondria in obesity and type 2 diabetes. *Diabetes* 54:8-14
25. **Petersen KF, Dufour S, Befroy D, Garcia R, Shulman GI** 2004 Impaired mitochondrial activity in the insulin-resistant offspring of patients with type 2 diabetes. *N Engl J Med* 350:664-671
26. **Rong JX, Qiu Y, Hansen MK, Zhu L, Zhang V, Xie M, Okamoto Y, Mattie MD, Higashiyama H, Asano S, Strum JC, Ryan TE** 2007 Adipose mitochondrial biogenesis is suppressed in db/db and high-fat diet-fed mice and improved by rosiglitazone. *Diabetes* 56:1751-1760
27. **Valerio A, Cardile A, Cozzi V, Bracale R, Tedesco L, Pisconti A, Palomba L, Cantoni O, Clementi E, Moncada S, Carruba MO, Nisoli E** 2006 TNF-alpha downregulates eNOS expression and mitochondrial biogenesis in fat and muscle of obese rodents. *J Clin Invest* 116:2791-2798
28. **Bogacka I, Ukropcova B, McNeil M, Gimble JM, Smith SR** 2005 Structural and functional consequences of mitochondrial biogenesis in human adipocytes in vitro. *J Clin Endocrinol Metab* 90:6650-6656
29. **Misra A, Garg A** 2003 Clinical features and metabolic derangements in acquired generalized lipodystrophy: case reports and review of the literature. *Medicine (Baltimore)* 82:129-146
30. **Handschin C, Spiegelman BM** 2006 Peroxisome proliferator-activated receptor gamma coactivator 1 coactivators, energy homeostasis, and metabolism. *Endocr Rev* 27:728-735
31. **Semple RK, Crowley VC, Sewter CP, Laudes M, Christodoulides C, Considine RV, Vidal-Puig A, O'Rahilly S** 2004 Expression of the thermogenic nuclear hormone receptor coactivator PGC-1alpha is reduced in the adipose tissue of morbidly obese subjects. *Int J Obes Relat Metab Disord* 28:176-179
32. **Tiraby C, Tavernier G, Lefort C, Larrouy D, Bouillaud F, Ricquier D, Langin D** 2003 Acquisition of brown fat cell features by human white adipocytes. *J Biol Chem* 278:33370-33376
33. **Tsukiyama-Kohara K, Poulin F, Kohara M, DeMaria CT, Cheng A, Wu Z, Gingras AC, Katsume A, Elchebly M, Spiegelman BM, Harper ME, Tremblay ML, Sonenberg**

- N 2001 Adipose tissue reduction in mice lacking the translational inhibitor 4E-BP1. *Nat Med* 7:1128-1132
34. **Pirinen E, Kuulasmaa T, Pietila M, Heikkinen S, Tusa M, Itkonen P, Boman S, Skommer J, Virkamaki A, Hohtola E, Kettunen M, Fatrai S, Kansanen E, Koota S, Niiranen K, Parkkinen J, Levonen AL, Yla-Herttuala S, Hiltunen JK, Alhonen L, Smith U, Janne J, Laakso M** 2007 Enhanced polyamine catabolism alters homeostatic control of white adipose tissue mass, energy expenditure, and glucose metabolism. *Mol Cell Biol* 27:4953-4967
 35. **Lehr L, Canola K, Asensio C, Jimenez M, Kuehne F, Giacobino JP, Muzzin P** 2006 The control of UCP1 is dissociated from that of PGC-1alpha or of mitochondriogenesis as revealed by a study using beta-less mouse brown adipocytes in culture. *FEBS Lett* 580:4661-4666
 36. **Ott V, Fasshauer M, Dalski A, Klein HH, Klein J** 2002 Direct effects of ciliary neurotrophic factor on brown adipocytes: evidence for a role in peripheral regulation of energy homeostasis. *J Endocrinol* 173:R1-8
 37. **Duplus E, Benelli C, Reis AF, Fouque F, Velho G, Forest C** 2003 Expression of phosphoenolpyruvate carboxykinase gene in human adipose tissue: induction by rosiglitazone and genetic analyses of the adipocyte-specific region of the promoter in type 2 diabetes. *Biochimie* 85:1257-1264
 38. **Kopecky J, Clarke G, Enerback S, Spiegelman B, Kozak LP** 1995 Expression of the mitochondrial uncoupling protein gene from the aP2 gene promoter prevents genetic obesity. *J Clin Invest* 96:2914-2923
 39. **Wellen KE, Hotamisligil GS** 2005 Inflammation, stress, and diabetes. *J Clin Invest* 115:1111-1119
 40. **Xu H, Barnes GT, Yang Q, Tan G, Yang D, Chou CJ, Sole J, Nichols A, Ross JS, Tartaglia LA, Chen H** 2003 Chronic inflammation in fat plays a crucial role in the development of obesity-related insulin resistance. *J Clin Invest* 112:1821-1830
 41. **Kim JY, van de Wall E, Laplante M, Azzara A, Trujillo ME, Hofmann SM, Schraw T, Durand JL, Li H, Li G, Jelicks LA, Mehler MF, Hui DY, Deshaies Y, Shulman GI, Schwartz GJ, Scherer PE** 2007 Obesity-associated improvements in metabolic profile through expansion of adipose tissue. *J Clin Invest* 117:2621-2637
 42. **Cinti S, Mitchell G, Barbatelli G, Murano I, Ceresi E, Faloia E, Wang S, Fortier M, Greenberg AS, Obin MS** 2005 Adipocyte death defines macrophage localization and function in adipose tissue of obese mice and humans. *J Lipid Res* 46:2347-2355
 43. **Lumeng CN, Deyoung SM, Bodzin JL, Saltiel AR** 2007 Increased inflammatory properties of adipose tissue macrophages recruited during diet-induced obesity. *Diabetes* 56:16-23

Figure Legends

Figure 1. CNTF reduces adipose tissue mass in obese mice. (A) Epididymal fat pad mass. *P<0.05 versus all other groups, **P<0.05 versus HFD. (B) Mean adipocyte area. *P<0.05 versus HFD. (C) Triglyceride content in adipose tissue. *P<0.05 versus HFD, # P<0.05 versus HFD PF. (D) Plasma leptin. *P<0.05 versus HFD, **P<0.05 versus Chow and HFD. (E) Distribution of adipocytes in epididymal fat pads with a representative cross section shown above. n=10 (Chow, CNTF), n=9 (HFD), n=7 (HFD PF).

Figure 2. Acute metabolic responses to CNTF treatment in adipocytes. Adipose tissue explants from epididymal fat were treated with CNTF and assessed for (A) lipolysis, (B) lipogenesis and (C) fatty acid oxidation. n=10 (Chow, CNTF), n=9 (HFD), n=7 (HFD PF). (D) 3T3 L1 adipocytes were treated with AICAR or CNTF for 5 h (closed bars) and fatty acid oxidation was assessed. n=9 for each condition from three experiments performed in triplicate. In other experiments, 3T3 L1 adipocytes were treated with CNTF for 3 days (open bars). The media was changed and adipocytes remained in CNTF-free media for 16 h after which fatty acid oxidation was assessed. AMPK Thr172 (E) and acetyl CoA carboxylase (ACC) Ser221 (E) phosphorylation was assessed in 3T3 L1 adipocytes treated acutely (45 min, closed bars) or for 3 days (open bars) with CNTF. (G) Triglyceride content was assessed by Oil Red O staining in 3T3-L1 adipocytes without (closed bars) or with (open bars) CNTF treatment for 3 days. n=6 for each condition from two experiments performed in triplicate. *P<0.05 versus Vehicle (for all figures).

Figure 3. Prolonged CNTF treatment reduces lipogenesis and increases fatty acid oxidation in adipocytes. C57Bl/6 mice were fed a Chow or high-fat diet (HFD) for 12 weeks. HFD mice were treated with CNTF for 10 days and another group were pair fed (HFD PF) to the CNTF group. Epididymal adipose tissue explants were removed from 4 h fasted mice and assessed for (A) lipolysis, (B) lipogenesis, (C) esterification into triglycerides and (D) fatty acid oxidation. n=10 (Chow, CNTF), n=9 (HFD), n=7 (HFD PF). *P<0.05 versus all other groups, **P<0.05 vs PF.

Figure 4. Prolonged CNTF treatment induces mitochondrial biogenesis. C57Bl/6J mice were fed a Chow or high-fat diet (HFD) for 12 weeks. HFD mice were treated with CNTF for 10 days and another group were pair fed (HFD PF) to the CNTF group. Epididymal adipose tissue was removed and electron microscopy revealed an increase in mitochondrial number (A) and no change in individual mitochondrial area (B). CNTF resulted in stable increases in NRF-1 (C), PGC-1 α (D) and CPT-1 (E) mRNA. Cytochrome C (F), ATP synthase α (G) and the 30 kDa Ip subunit (H) protein expression were enhanced by CNTF. n=10 (Chow, CNTF), n=9 (HFD), n=7 (HFD PF). *P<0.05 versus all other groups, # P<0.05 versus Chow and HFD PF.

Figure 5. p38 MAPK mediates the increase in CNTF-induced PGC-1 α content in 3T3-L1 adipocytes. (A) PGC-1 α mRNA was increased in 3T3-L1 adipocytes treated with CNTF for 5 h or 3 days. (B) p38 MAPK phosphorylation is increased with CNTF and inhibited by prior treatment with the compound SB202190 or p38 MAPK dominant negative expression. (C) AMPK Thr172 phosphorylation is increased by CNTF and is unaffected by SB202190 or p38 MAPK dominant negative expression. Representative blots are from the same immunoblot. The CNTF-induced increase in PGC-1 α mRNA is blocked by SB202190 (D) and p38 MAPK dominant negative expression (E). Experiments were performed in triplicate on 2 occasions (total n=6). *P<0.05 versus Vehicle, ** P<0.05 versus Vehicle and CNTF, # P<0.05 versus p38DN CNTF.

Figure 6. Low dose CNTF does not induce proinflammatory signaling in 3T3-L1 adipocytes. (A) IL-6 gene expression was not increased in adipocytes treated with 10 ng/ml CNTF. In other experiments, 3T3-L1 adipocytes were treated with various concentrations of CNTF and the media was collected for IL-6 (B) and TNF α (C) release. Experiments were performed in triplicate on 2 occasions (total n=6). *P<0.05 versus 0 ng/ml CNTF.

Table 1. CNTF and dietary effects on body mass, blood chemistry and mRNA content in adipose tissue

| | Chow | HFD | HFD PF | HFD CNTF |
|----------------------|-------------|-------------|---------------|-----------------|
| Pre-Mass (g) | 29.9 ± 0.6 | 33.6 ± 1.4* | 31.0 ± 0.8** | 31.9 ± 0.5** |
| Post-Mass (g) | 28.8 ± 0.5 | 33.1 ± 1.3* | 25.4 ± 0.3** | 26.2 ± 0.6** |
| Mass (% change) | -3.8 ± 0.7 | -1.3 ± 0.6 | -17.9 ± 1.9** | -17.9 ± 1.1** |
| Food Intake (kJ/day) | 15.8 ± 1.04 | 16.3 ± 0.4 | 6.2 ± 0.6* | 6.9 ± 0.7* |
| Blood glucose (mM) | 9.1 ± 0.6 | 12.2 ± 0.7* | 9.4 ± 0.7 | 10.6 ± 1.4 |
| Plasma insulin (pM) | 48 ± 17 | 164 ± 44* | 71 ± 22 | 59 ± 17 |
| Plasma NEFA (μM) | 651 ± 159 | 1120 ± 415 | 824 ± 91 | 400 ± 51* |
| CEBPα | 1.0 ± 0.1 | 1.3 ± 0.3 | 1.3 ± 0.2 | 1.6 ± 0.2** |
| PPARγ | 1.0 ± 0.2 | 1.4 ± 0.3 | 1.3 ± 0.3 | 1.8 ± 0.2** |
| UCP1 | 1.0 ± 0.1 | 0.6 ± 0.2 | 2.0 ± 0.4* | 0.8 ± 0.2 |
| UCP2 | 1.0 ± 0.2 | 0.7 ± 0.2 | 0.6 ± 0.2 | 0.8 ± 0.1 |
| UCP3 | 1.0 ± 0.3 | 0.8 ± 0.2 | 0.6 ± 0.3 | 1.0 ± 0.2 |
| CD68 | 1.0 ± 0.1 | 2.1 ± 0.5** | 2.1 ± 0.1** | 1.8 ± 0.3** |
| F4/80 | 1.0 ± 0.2 | 2.4 ± 0.3** | 2.2 ± 0.2** | 1.7 ± 0.2** |

* P<0.05 versus all other groups, ** P<0.05 versus Chow

Table 2. CNTF-induced suppression of lipogenic gene expression in C57Bl/6 mouse adipose tissue.

| Gene name | Gene Symbol | Fold Change |
|--|--------------------|--------------------|
| Acyl-CoA synthetase long-chain family member 1 | Acsl1 | 1.52 |
| Acyl-CoA synthetase long-chain family member 4 | Acsl4 | 1.61 |
| Acyl-CoA synthetase medium-chain family member 1 | Acsm1 | 3.13 |
| Diacylglycerol acyltransferase 1 | Dgat1 | 2.21 |
| Fatty acid desaturase 1 | Fads1 | 1.75 |
| Fatty acid synthase | Fasn | 1.74 |
| Fatty acid tranlocase / CD36 | | 1.95 |
| Glycerol-3-phosphate acyltransferase | Gpam | 1.85 |
| Pyruvate carboxylase | Pcx | 1.85 |
| Phosphoenolpyruvate carboxykinase 1, cytosolic | Pck1 | 2.24 |
| Stearoyl-Coenzyme A desaturase 1 | Scd1 | 1.64 |

Figure 1

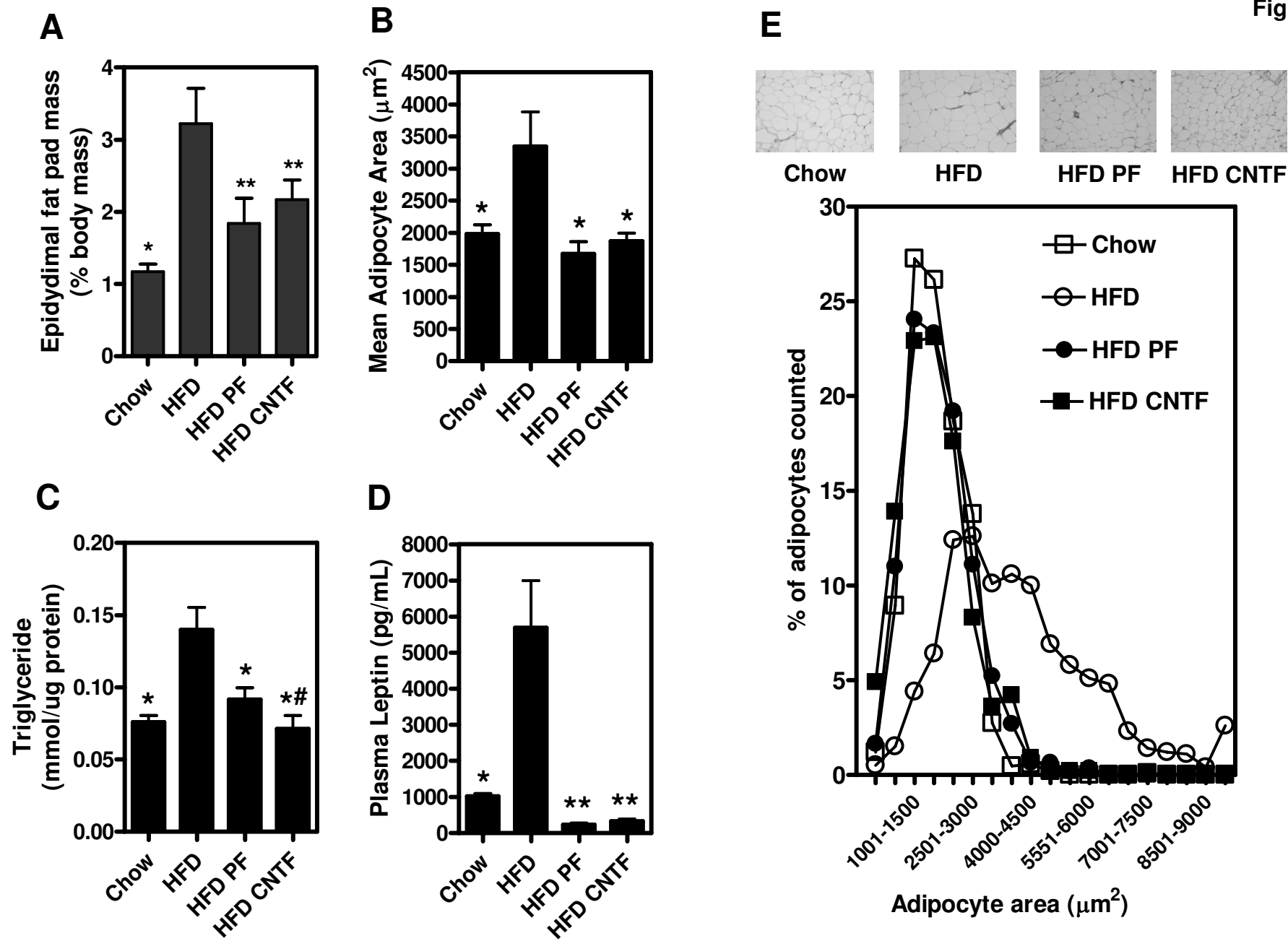


Figure 2

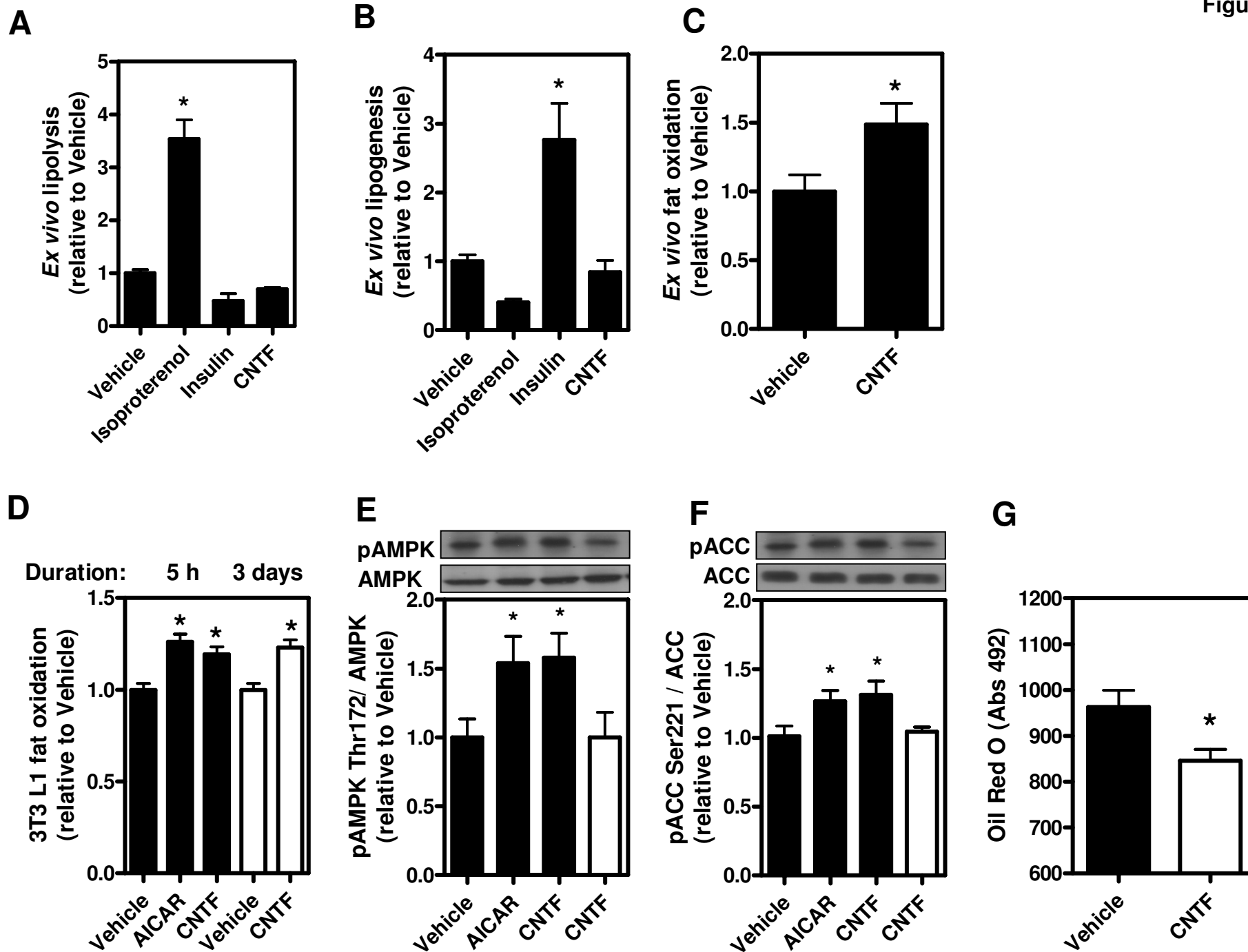


Figure 3

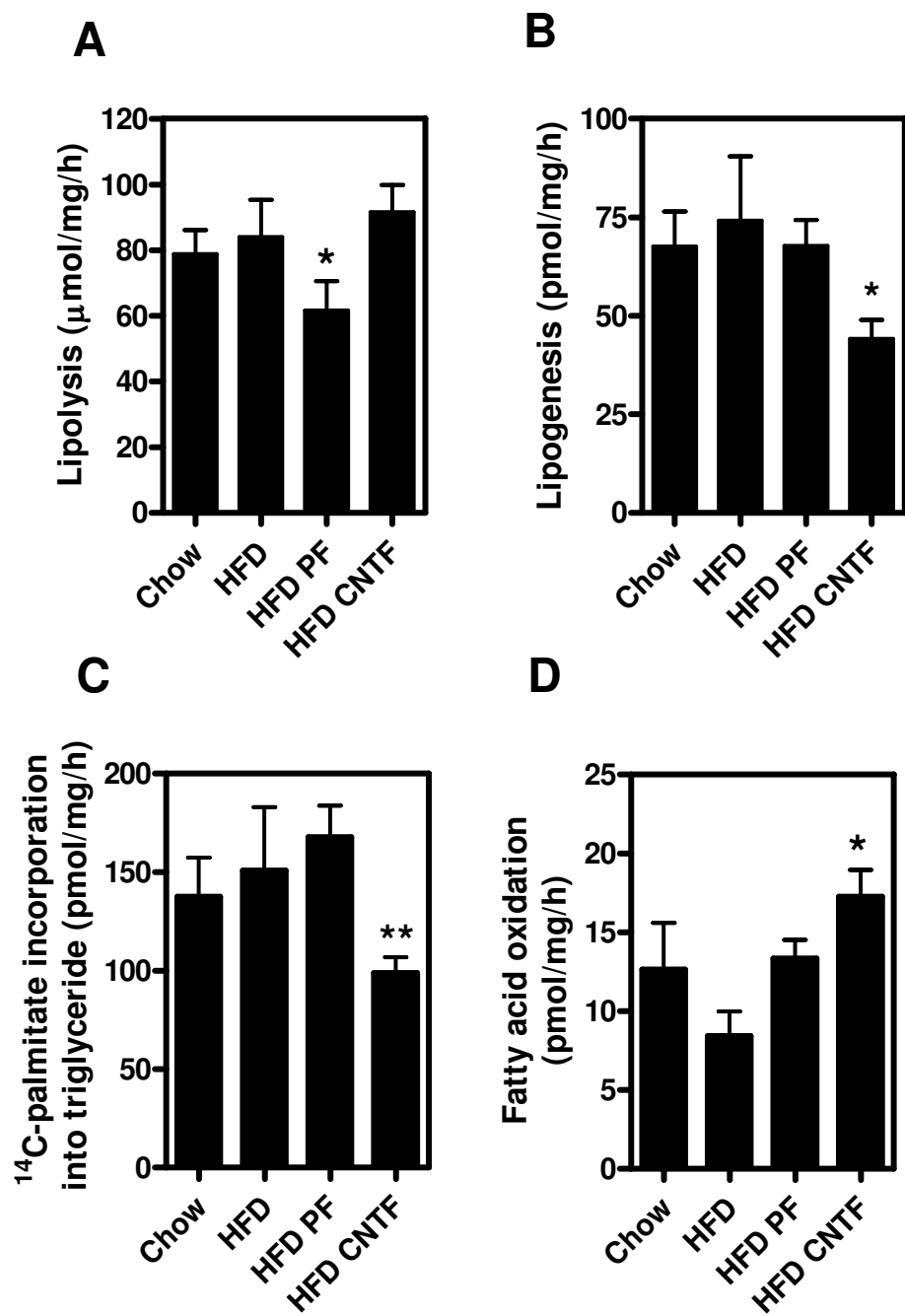


Figure 4

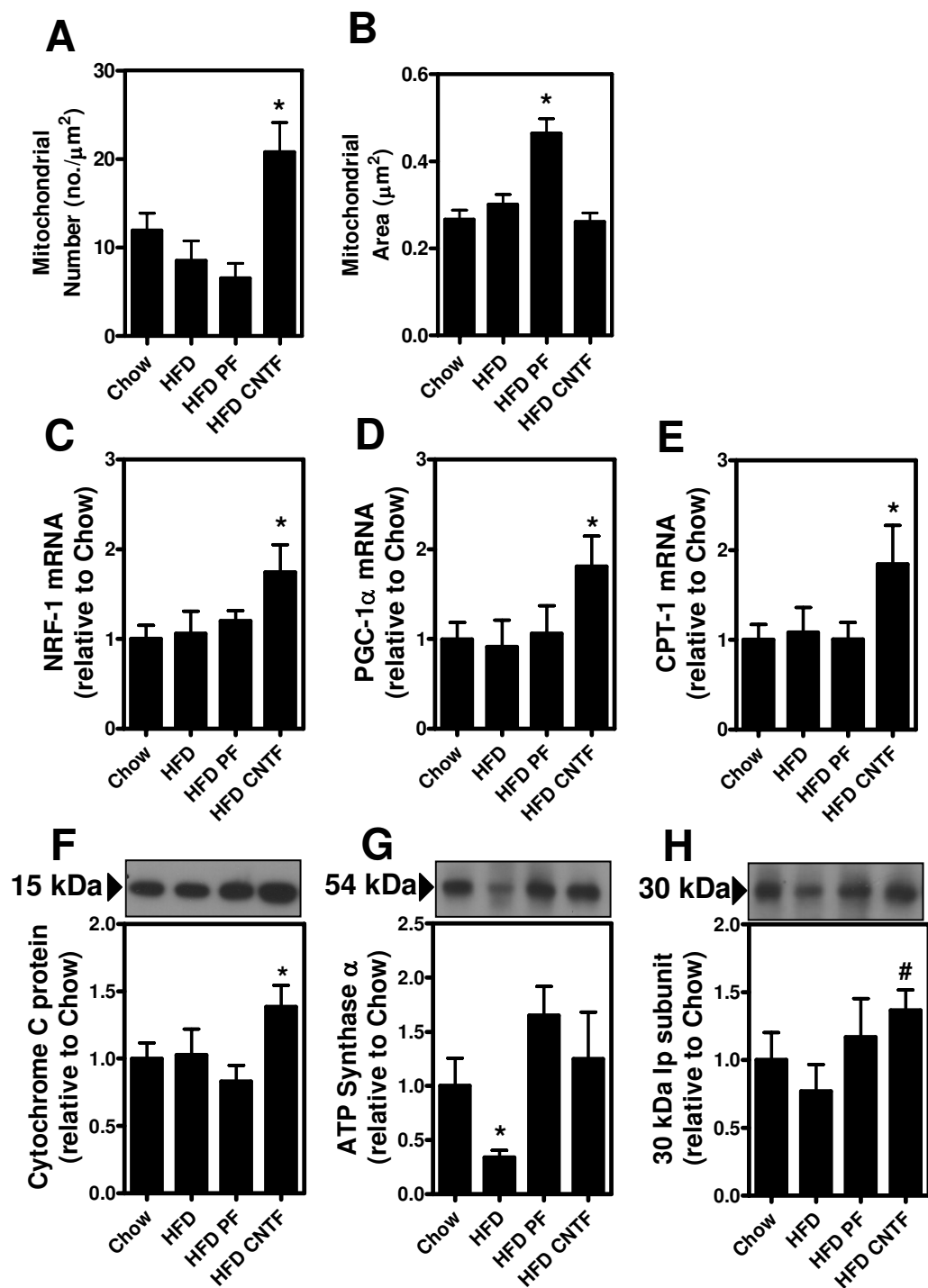


Figure 5

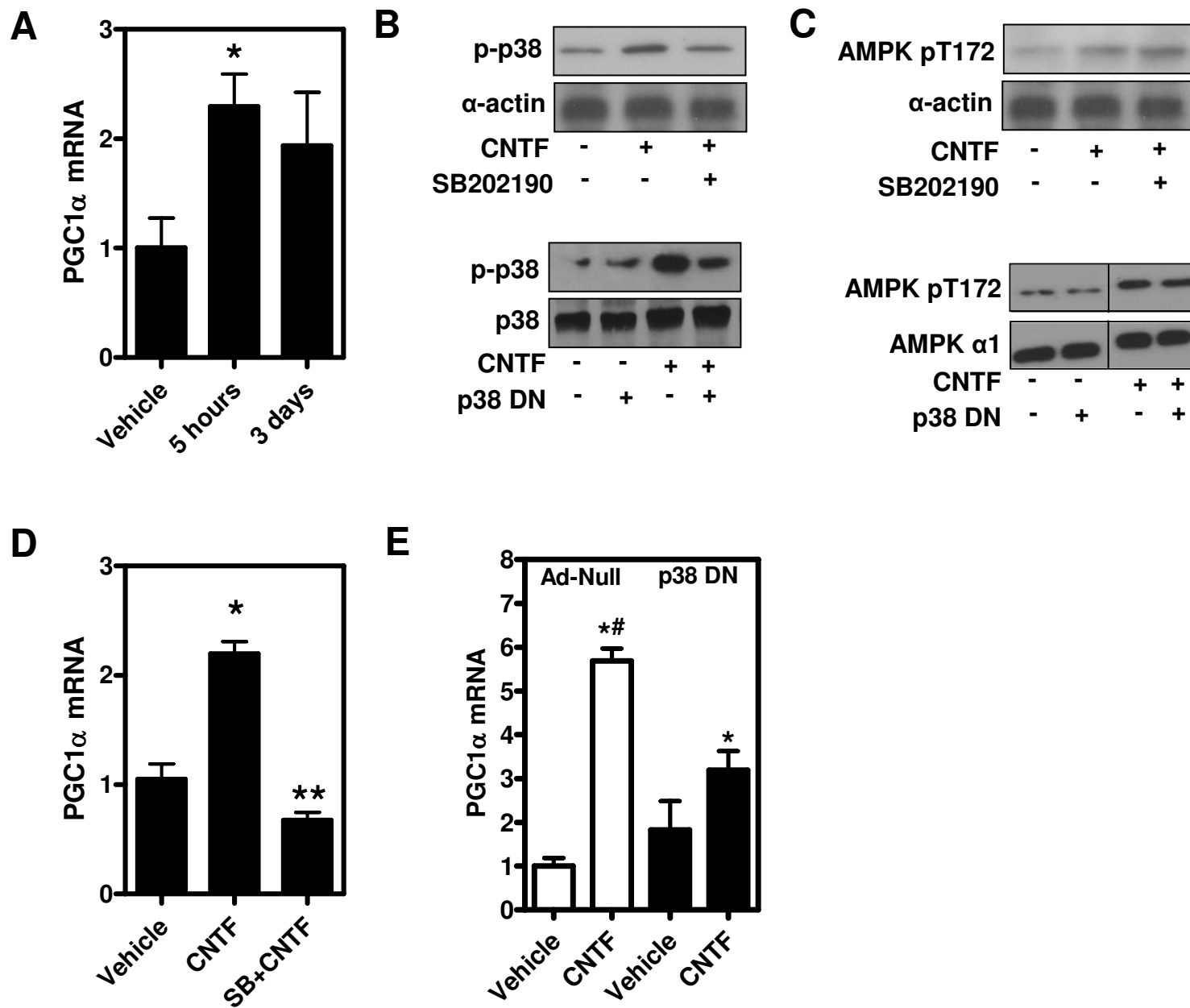


Figure 6

